NANO LETTERS

2008
Vol. 8, No. 9
3004-3009

Controlled Synthesis of Millimeter-Long Silicon Nanowires with Uniform Electronic Properties

Won Il Park,*,† Gengfeng Zheng,‡ Xiaocheng Jiang,‡ Bozhi Tian,‡ and Charles M. Lieber*,‡,§

Division of Materials Science and Engineering, Hanyang University, Seoul 133-791, Korea, and Department of Chemistry and Chemical Biology, and School of Engineering and Applied Sciences, Harvard University, Cambridge, Massachusetts 02138

Received July 12, 2008; Revised Manuscript Received August 6, 2008

ABSTRACT

We report the nanocluster-catalyzed growth of ultralong and highly uniform single-crystalline silicon nanowires (SiNWs) with millimeter-scale lengths and aspect ratios up to approximately 100 000. The average SiNW growth rate using disilane (Si_2H_6) at 400 °C was 31 μm/min, while the growth rate determined for silane (SiH_4) reactant under similar growth conditions was 130 times lower. Transmission electron microscopy studies of millimeter-long SiNWs with diameters of 20−80 nm show that the nanowires grow preferentially along the ⟨110⟩ direction independent of diameter. In addition, ultralong SiNWs were used as building blocks to fabricate one-dimensional arrays of field-effect transistors (FETs) consisting of approximately 100 independent devices per nanowire. Significantly, electrical transport measurements demonstrated that the millimeter-long SiNWs had uniform electrical properties along the entire length of wires, and each device can behave as a reliable FET with an on-state current, threshold voltage, and transconductance values (average ±1 standard deviation) of 1.8 ± 0.3 μA, 6.0 ± 1.1 V, 210 ± 60 nS, respectively. Electronically uniform millimeter-long SiNWs were also functionalized with monoclonal antibody receptors and used to demonstrate multiplexed detection of cancer marker proteins with a single nanowire. The synthesis of structurally and electronically uniform ultralong SiNWs may open up new opportunities for integrated nanoelectronics and could serve as unique building blocks linking integrated structures from the nanometer through millimeter length scales.

Semiconducting nanowires (NWs)[1−5] are attractive building blocks for fabricating functional nanodevices with single device demonstrations reported for field-effect transistors (FETs),[6] memories,[7] light emitting diodes,[8] laser diodes,[9] and biological sensors.[10] More complex device arrays and simple circuits, including logic gates,[11] ring oscillators,[12] and multiplexed biosensors,[13] have been demonstrated by interconnection of multi-NW devices. A complementary approach for device integration would be to employ ultralong NWs with multiple devices on a single NW, assuming that materials with uniform structure and electronic properties could be prepared. Ultralong nanowires could also benefit overall integration by facilitating interconnection of nanoelectronic device arrays, which are defined on single NWs, to larger scale input/output wires in a system.

Previously, millimeter-long SiNWs[14] with a range of structural properties have been produced by high-temperature thermal evaporation of silicon monoxide[14a] and silicon[14b] powders; however, the electronic properties and nanoelectronic device characteristics have not been reported. The nanocluster-catalyzed vapor−liquid−solid (VLS) growth method is a promising method for the growth of single-crystal NWs with controlled diameter, length, and electronic properties.[1−4] The kinetics of SiNW VLS growth have been studied recently by several groups.[15,16] Interestingly, diameter-independent[15] and diameter-dependent[16] growth rates have been observed, although in all cases the rates have been slower than 1−2 μm/min.[17] These reported rates make the VLS-based growth of millimeter length SiNWs a significant challenge. We note that much larger micrometer-scale diameter Si whiskers have exhibited growth rates reaching ∼1 μm/sec,[18] which would facilitate growth of millimeter length structures.

To investigate nanocluster-catalyzed VLS synthesis of millimeter-long single-crystal SiNWs, we have considered whether the overall growth rate could be increased by accelerating the rate-limiting step in the process.[15,16,19,20] The overall growth process can be broken down into contributions from (i) catalytic adsorption of gaseous reactants at the

* Corresponding author. E-mail: wipark@hanyang.ac.kr (W.I.P) and cml@cmliris.harvard.edu (C.M.L.).
† Hanyang University.
‡ Department of Chemistry and Chemical Biology, Harvard University.
§ Division of Engineering and Applied Science, Harvard University.

10.1021/nl802063q CCC: $40.75
Published on Web 08/19/2008

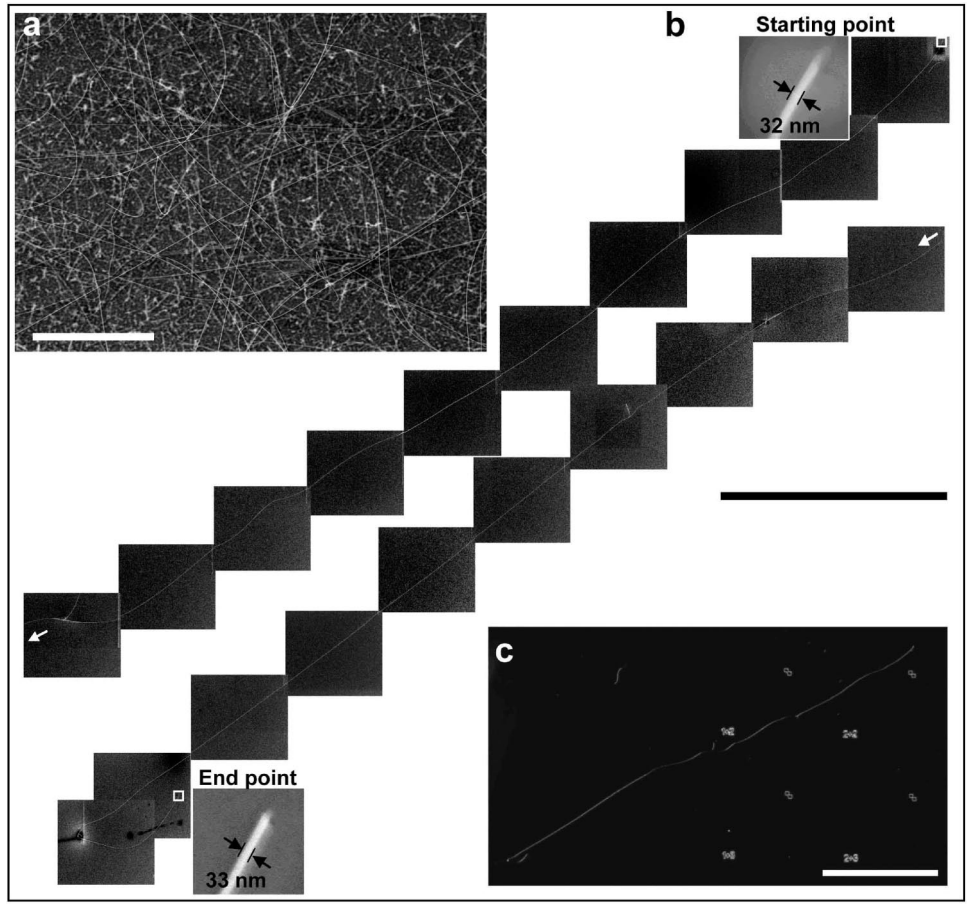

Figure 1. (a) SEM image of as-grown ultralong SiNWs synthesized by Si_2H_6 at 400 °C for 30 min. Scale bar, 20 μm. (b) A series of 20 SEM images of a 2.3 mm- long SiNW transferred on SiO_2/Si substrate. Scale bar, 200 μm. Insets, SEM images of starting and end segments of this NW. (c) Dark-field optical image of the same wire. Scale bar, 500 μm.

surface of liquid nanoparticles, (ii) diffusion of Si through the liquid alloy to a sink, and (iii) crystallization at liquid−solid interface.[2,16,19,21] The critical importance of steps (i) and/or (iii) in limiting growth rate has been discussed.[15,16,19,20] Our previous studies have shown that single-crystal SiNWs synthesized via gold nanocluster-catalyzed VLS growth proceeds with growth rates of approximately 1 μm/min using silane (SiH_4) as gas-phase recactant.[17,22] The strong temperature dependence of the SiNW growth rate under optimized conditions suggests that SiH_4 decomposition kinetics are more important than the gas-phase mass transport[23] and thus that acceleration of the decomposition step might enhance the observed growth rate. Here, we explore SiNW growth using disilane (Si_2H_6) since Si_2H_6 is expected to have a higher catalytic decomposition rate due to lower activation energy for cleavage of Si−Si versus Si−H bonds.[24]

SiNWs were synthesized at 390−410 °C using gold nanoclusters as catalysts and Si_2H_6 (3 sccm) as reactant source[25] with other procedures similar to our previous reports for SiH_4-based SiNW growth.[4,17,22,26] Scanning electron microscopy (SEM) images of the growth wafer (Figure 1a) show the presence of very long nanowires with varying degrees of entanglement. The long SiNWs were transferred to clean substrates via a reported shear contact printing process,[27] which can extend and align the SiNWs for direct and unambiguous length measurements. Analysis of a series of 20 scanning SEM images recorded along the length of a representative ultralong SiNW (Figure 1b) demonstrate several important points. First, the length of the approximately 30 nm diameter nanowire, 2.3 mm, is almost 100 times longer than the SiNWs we typically produce using SiH_4 reactant. The entire SiNW can also be readily visualized in dark-field optical microscopy images as shown in Figure 1c. Second, the NW diameter is very uniform with the starting and end points of approximately 31 and 33 nm, respectively. This uniform diameter indicates (i) that there is little or no homogeneous deposition of Si_2H_6 on the elongating nanowire during the synthesis[26] and (ii) that Au from the catalyst does not incorporate into or diffuse along the surface to a substantial amount during growth. Third, quantitative analysis of the lengths of ultralong SiNWs produced following 1 h growth yielded an average of 1.8 mm with longest NWs at or exceeding 3.5 mm.

We have compared SiNW growth rates using Si_2H_6 versus SiH_4 with other conditions fixed except growth temperature in order to probe the origin of the faster growth rates leading to the ultralong SiNWs. Plots of the SiNW length versus growth time with Si_2H_6 at 400 °C, SiH_4 at 400 °C, and SiH_4 at 450 °C for 30 nm diameter NWs (Figure 2a) show that the average growth rate for Si_2H_6 at 400 °C is approximately 31 μm/min, which is approximately 130 times higher than that for SiH_4 at the same temperature (0.24 μm/min) and 31

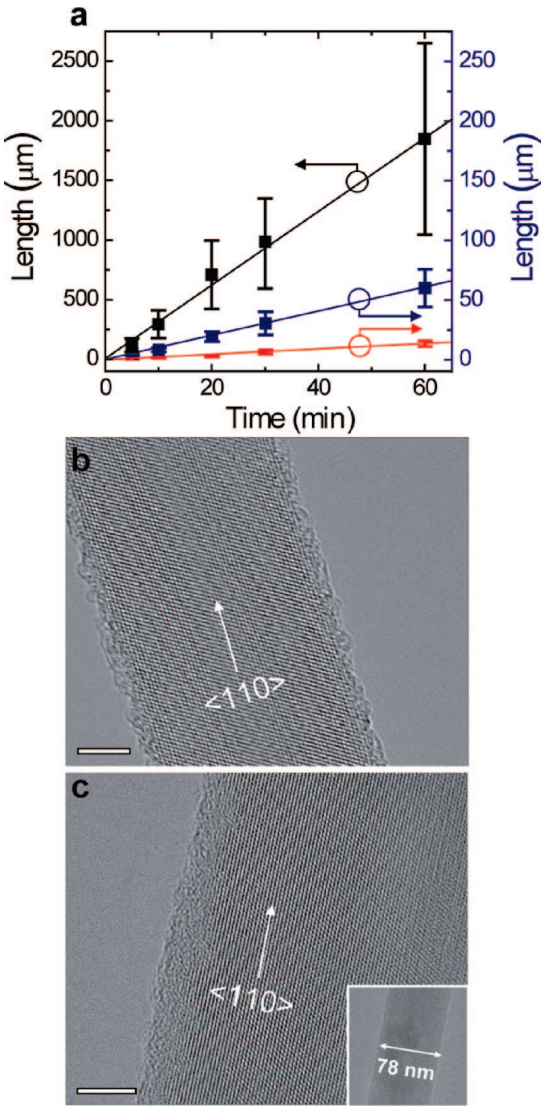

Figure 2. (a) Plot of SiNW length versus growth time for Si_2H_6 at 400 °C (black), SiH_4 at 400 °C (red) and SiH_4 450 °C (blue). (b) Lattice-resolved TEM image recorded along ⟨111⟩ zone axis of a 18 nm diameter ultralong SiNW; scale bar is 5 nm. (c) Lattice-resolved TEM image of a 78 nm diameter ultralong SiNW; scale bar is 5 nm. Inset is a lower magnification image of the SiNW.

times higher than for SiH_4 at our optimal growth temperature of 450 °C (1.0 μm/min). Using the temperature-dependent gas phase decomposition rate data for Si_2H_6 and SiH_4,[24] we estimate Si_2H_6 (400 °C):SiH_4 (400 and 450 °C) of approximately 170 and 10, respectively. These values are similar to the experimental ratios of growth rates and thus suggest that reactant decomposition kinetics is important in determining the observed SiNW growth rates.

The structural characteristics of the ultralong SiNWs were also investigated by transmission electron microscopy (TEM). Lattice-resolved images of an approximately 18 nm diameter SiNW (Figure 2b) show that the SiNW is a single-crystalline structure despite the fact that growth occurred at rates at least 10 times greater than previous studies.[4,15−17,19,22] The TEM image and two-dimensional Fourier transform analysis (Supporting Information, Figure S1a) further demonstrated that the growth axis was ⟨110⟩, consistent with previous studies of smaller diameter SiNWs.[4,22] In addition, TEM studies of 18 SiNWs with diameters from 15 to 80 nm (Figure 2c and Supporting Information, Figure S1b) all showed single-crystalline structures with a growth axis of ⟨110⟩ independent of diameter, where 13/18 of the sampled SiNWs had diameters between 29 to 80 nm. Interestingly, the diameter-independent growth direction observed for the ultralong SiNWs contrasts previous studies where a cross-over to ⟨111⟩ direction at approximately 20 nm was observed.[4,5,22]

Previously, Schmidt et al.[5] proposed a model based on the free energy, which is influenced by the interplay of the liquid−solid interfacial tension with Si surface edge tension, to explain consistently diameter dependent growth in SiNWs. Within the context of this model, a larger critical cross-over diameter from ⟨110⟩ to ⟨111⟩ would be observed for an interfacial thickness that increased with crystallization rate. We speculate that the faster growth rates used to achieve the ultralong SiNWs might lead to an increase of the interfacial thickness parameter, although future studies of critical diameter versus growth rate will be required to clarify this point. Regardless of the detailed origin, we believe these observations suggest that it will be interesting to explore and possibly exploit kinetic effects as a means to controlling growth directions for NWs produced by the nanocluster-catalyzed VLS process.

The ultralong SiNWs represent potentially attractive building blocks for nanoelectronics because it would be possible to define a large number of devices on a single NW, thus facilitating integration as shown schematically in Figure 3a. In addition, the fabrication and characterization of multiple devices on a single NW could provide important information addressing doping and electronic uniformity of these nanostructures. To address these issues, we have prepared ultralong boron-doped SiNWs,[25] aligned the NWs on substrate by shear contact printing,[27] and defined arrays of FETs by electron beam lithography.[10a,11,26,28] A representative optical image (Figure 3b) highlights the large number of addressable FETs defined on the ultralong SiNWs.

Electrical transport measurements showed that more than 90% devices behaved as good *p*-type devices. Specifically, source−drain current (I_D) versus source−drain voltage (V_D) curves at small V_D were linear, which demonstrates good contacts across the NW. The decrease in I_D with increasingly positive V_G (Figure S2) also showed that devices were *p*-type depletion mode FETs. In addition, we have assessed and compared quantitatively key transistor characteristics, including on-state current, I_{on}, peak transconductance, G_M, and threshold voltage, V_{th}, as a function of position across the single SiNW array. Notably, the I_{on} (Figure 3c), G_M (Figure 3d), and V_{th} (Figure 3e) show very reproducible values across the entire array spanning almost 1 mm in length with average ±1 standard deviation values of 1.77 ± 0.33 μA, 213 ± 61 nS, and 6.0 ± 1.1 V, respectively. Previous studies of individual nanowire FETs[6a,29] have exhibited larger variations in key FET properties, with variations in threshold voltage of 35−135% versus ∼20% and transconductance of 58−76% versus ∼30%. This comparison indicates that the ultralong

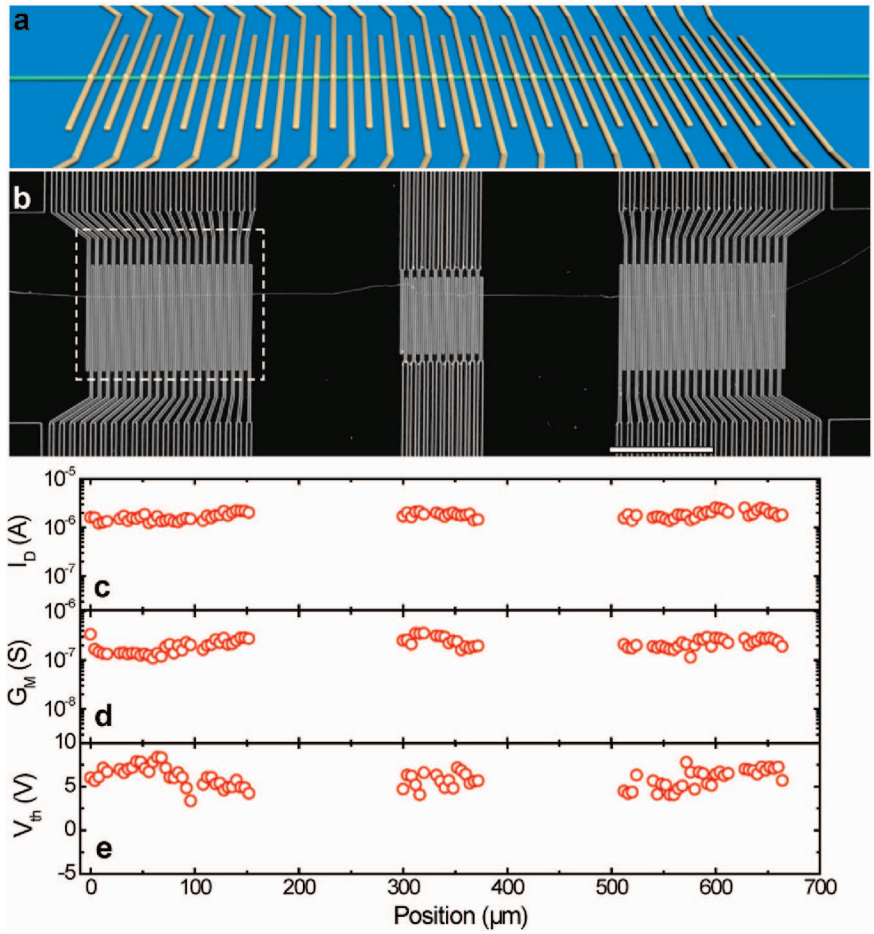

Figure 3. (a) Schematic of multiple FET array on a single ultralong *p*-SiNW. (b) Dark-field optical image of multiple FETs defined by electron beam lithography. The *p*-SiNW is horizontal in the image and the vertical lines crossing the NW correspond to S/D electrodes with 2 μm width/2 μm separation; scale bar is 100 μm. The dashed white rectangle corresponds to a similar area shown schematically in (a). (c) Position vs I_D at $V_D = 1$ V and $V_G = -10$ V measured from the multiple FETs defined on the single *p*-SiNW in the image. (d) Position vs G_M at $V_D = 1$ V. (e) Position vs V_{th}.

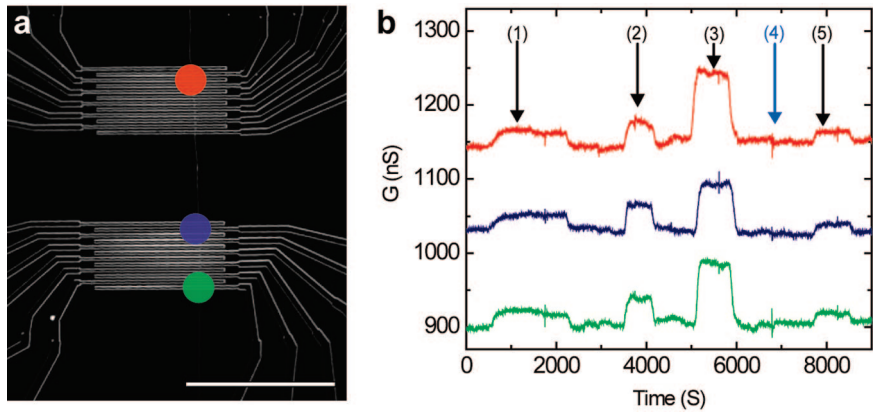

Figure 4. (a) Optical image of a multiple sensor array with similar source-drain dimensions as in Figure 3b; scale bar, 100 μm. The red, blue, and green circles highlight regions from which sensing data were recorded. (b) Conductance-versus-time data measured simultaneously from three FET devices from the red, blue, and green regions of the device array. The SiNW FET array was functionalized with mAb for PSA, and the data were recorded by alternating delivery of target solutions (PSA or BSA) and buffer solution where vertical arrows correspond to the delivery of (1) 20 pg/ml PSA, (2) 500 pg/ml PSA, (3) 10 ng/ml PSA, (4) 10 μg/ml BSA, and (5) 20 pg/ml PSA solutions. The functionalization and measurement procedures were the same as reported previously.[13,17]

SiNWs are electrically homogeneous and yield device reproducibility higher than achieved from single NW-based FETs. Last, these measurements also suggest that the active boron dopant yielding the *p*-type behavior must be incorporated in a uniform manner during nanocluster-catalyzed VLS growth.

The ability to define large numbers of functional FETs along single ultralong NWs can open up new opportunities

for integrated nanoelectronics. To demonstrate this concept, we have explored multiplexed protein detection using monoclonal antibody (mAb) functionalized SiNW FETs (Figure 4a). In previous studies,[13] we have demonstrated multiplexed detection using mAb functionalized devices, but in this case, each device was from an individual SiNW thus necessitating well-defined assembly to achieve the FET array. Demonstration of multiplexed measurements from independently addressable FETs defined on a single ultralong SiNW has not been previously achieved using either nanowires or carbon nanotubes. However, this approach could have substantial impact on the biosensor area[10a,13] because it (i) simplifies fabrication of multiplexed sensor device arrays and, given the greater device homogeneity for FETs defined on a single ultralong SiNW, (ii) opens up the opportunity to assess sensing reproducibility in device arrays where device-to-device variability should not be the dominating factor.

Conductance versus time data recorded from three distinct FETs defined on the single ultralong SiNW, which was functionalized uniformly with the mAb for prostate specific antigen (PSA), showed several key features. First, the devices exhibited well-defined and reversible conductance increases associated with the binding and unbinding of the specific target PSA. Second, the conductance change was proportional to the PSA concentration, as expected for equilibrium binding response. Third, the concentration-dependent conductance change recorded in the distinct FET elements, which were separated by >100 μm, was similar and testifies to the electronic uniformity of the ultralong SiNWs and the uniform mAb functionalization. Fourth, we note that addition bovine serum albumin at 1000 times higher concentration showed no response, demonstrating good selectivity.[13] Last, the reproducible conductance change from each of the addressable devices is consistent with the homogeneous device characteristics demonstrated in Figure 3. While the present measurements represent a relatively simple demonstration of multiplex protein detection, they do demonstrate a new approach for multiplexing that could be extended in the future to include parallel, real-time measurements from a larger number of devices functionalized with diverse mAb receptors.

In summary, we have demonstrated the nanocluster-catalyzed growth of millimeter-long and highly uniform single-crystalline SiNWs with aspect ratios up to approximately 100 000. The average SiNW growth rates using Si_2H_6 reactant were 30−130 times faster than previous rates observed using SiH_4 reactant under similar growth conditions. TEM studies showed that the ultralong SiNWs grow preferentially along the ⟨110⟩ direction, independent of diameter, and suggest that kinetic effects may be used as a means for controlling growth directions in NWs produced by the nanocluster-catalyzed VLS process. In addition, ultralong SiNWs were used as building blocks to fabricate one-dimensional FET arrays that exhibit high-degree of device uniformity over millimeter dimensions and testify to the electrical/doping homogeneity of SiNWs produced by nanocluster-catalyzed VLS growth. Lastly, the uniform device properties of one-dimensional FET arrays were exploited to demonstrate a new approach to multiplexed detection of cancer marker proteins with a single nanowire. The synthesis of structurally and electronically uniform ultralong SiNWs may open up new opportunities for integrated nanoelectronics and could serve as unique building blocks linking integrated structures from the nanometer through millimeter length scales.

Acknowledgment. We thank J. Xiang for helpful discussion. W.I.P acknowledges support from the Korea Research Foundation Grant funded by the Korean Government (MOE-HRD, Basic Research Promotion Fund; KRF-2007-331-D00194). C.M.L. acknowledges support of this work through a contract from National Institutes of Health, MITRE Corporation, and Samsung Electronics.

Supporting Information Available: Two-dimensional Fourier transforms and source−drain current versus gate voltage curves. This material is available free of charge via the Internet at http://pubs.acs.org.

References

(1) Morales, A.; Lieber, C. M. *Science* **1998**, *279*, 208.
(2) (a) Lieber, C. M.; Wang, Z. L. *MRS Bull.* **2007**, *32*, 99. (b) Xia, Y.; Yang, P.; Sun, Y.; Wu, Y.; Mayers, B.; Gates, B.; Yin, Y.; Kim, F.; Yan, H. *Adv. Mater.* **2003**, *15*, 353. (c) Thelander, C.; Agarwal, P.; Brongersma, S.; Eymery, J.; Feiner, L. F.; Forchel, A.; Scheffler, M.; Riess, W.; Ohlsson, B. J.; Gosele, U.; Samuelson, L. *Mater. Today* **2006**, *9*, 28.
(3) Schmidt, V.; Gösele, U. *Science* **2007**, *316*, 698.
(4) Wu, Y.; Cui, Y.; Huynh, L.; Barrelet, C. J.; Bell, D. C.; Lieber, C. M. *Nano Lett.* **2004**, *4*, 433.
(5) Schmidt, V.; Senz, S.; Gösele, U. *Nano Lett.* **2005**, *5*, 931.
(6) (a) Cui, Y.; Zhong, Z. H.; Wang, D. L.; Wang, W. U.; Lieber, C. M. *Nano Lett.* **2003**, *3*, 149. (b) Xiang, J.; Lu, W.; Hu, Y.; Wu, Y.; Yan, H.; Lieber, C. M. *Nature* **2006**, *441*, 489. (c) Ng, H. T.; Han, J.; Yamada, T.; Nguyen, P.; Chen, Y. P.; Meyyappan, M. *Nano Lett.* **2004**, *4*, 1247. (d) Park, W. I.; Kim, J. S.; Yi, G.-C.; Lee, H. J. *Adv. Mater.* **2005**, *17*, 1393.
(7) Lu, W.; Lieber, C. M. *Nat. Mater.* **2007**, *6*, 841.
(8) (a) Duan, X.; Huang, Y.; Cui, Y.; Wang, J.; Lieber, C. M. *Nature* **2001**, *409*, 66. (b) Zhong, Z.; Qian, F.; Wang, D.; Lieber, C. M. *Nano Lett.* **2003**, *3*, 343. (c) Huang, Y.; Duan, X.; Lieber, C. M. *Small* **2005**, *1*, 142. (d) Qian, F.; Li, Y.; Gradeèak, S.; Barrelet, C. J.; Wang, D.; Lieber, C. M. *Nano Lett.* **2004**, *4*, 1975.
(9) Duan, X.; Huang, Y.; Agarwal, R.; Lieber, C. M. *Nature* **2003**, *421*, 241.
(10) (a) Cui, Y.; Wei, Q.; Park, H.; Lieber, C. M. *Science* **2001**, *293*, 1289. (b) Hahm, J.; Lieber, C. M. *Nano Lett.* **2004**, *4*, 51. (c) Shim, M.; Kam, N. W. S.; Chen, R. J.; Li, Y. M.; Dai, H. J. *Nano Lett.* **2002**, *2*, 285.
(11) Huang, Y.; Duan, X.; Cui, Y.; Lauhon, L. J.; Kim, K.; Lieber, C. M. *Science* **2001**, *294*, 1313.
(12) Friedman, R. S.; McAlpine, M. C.; Ricketts, D. S.; Ham, D.; Lieber, C. M. *Nature* **2005**, *434*, 1085.
(13) Zheng, G.; Patolsky, F.; Cui, Y.; Wang, W. U.; Lieber, C. M. *Nat. Biotechnol.* **2005**, *23*, 1294.
(14) (a) Shi, W. S.; Peng, H. Y.; Zheng, Y. F.; Wang, N.; Shang, N. G.; Pan, Z. W.; Lee, C. S.; Lee, S. T. *Adv. Mater.* **2000**, *12*, 1343. (b) Shi, Y.; Hu, Q.; Araki, H.; Suzuki, H.; Gao, H.; Yang, W.; Noda, T. *Appl. Phys. A: Mater. Sci. Process.* **2005**, *80*, 1733.
(15) Kodambaka, S.; Tersoff, J.; Reuter, M. C.; Ross, F. M. *Phys. Rev. Lett.* **2006**, *96*, 096105.
(16) Schmidt, V.; Senz, S.; Gösele, U. *Phys. Rev. B* **2007**, *75*, 045335.
(17) Patolsky, F.; Zheng, G.; Lieber, C. M. *Nat. Protocols* **2006**, *1*, 1711.
(18) Nebol'sin, V. A.; Shchetinin, A. A.; Dolgachev, A. A.; Korneeva, V. V. *Inorg. Mater.* **2005**, *41*, 1256.
(19) Givargizov, E. I. *J. Cryst. Growth* **1975**, *31*, 20.
(20) Bootsma, G. A.; Gassen, H. J. *J. Cryst. Growth* **1971**, *10*, 223.
(21) Wu, Y.; Yang, P. *J. Am. Chem. Soc.* **2001**, *123*, 3165.
(22) Cui, Y.; Lauhon, L. J.; Gudiksen, M. S.; Wang, J.; Lieber, C. M. *Appl. Phys. Lett.* **2001**, *78*, 2214.

(23) Masi, M.; Cavallotti, C.; Carrà, S. In *Silicon-Based Materials and Devices*; Nalwa, H. S., Eds.; Academic Press: San Diego, 2001; Ch. 4.
(24) Roenigk, K. F.; Jensen, K. F.; Carr, R. W. *J. Phys. Chem.* **1987**, *91*, 5732.
(25) SiNWs were synthesized at 390−410 °C using well-dispersed gold nanoclusters (10−80 nm diameter) as catalysts, H_2 as carrier gas (10 cm^3 at standard temperature and pressure, STM min^{-1}) and Si_2H_6 (3 STM min^{-1}) as reactant source at 10 torr. Boron-doped *p*-type SiNWs were synthesized using 100 ppm B_2H_6 as doping source with a Si_2H_6/B_2H_6 ratio of $10^5-2 \times 10^5$:1 (Si/B = $10^5-2 \times 10^5$:1).
(26) Yang, C.; Zhong, Z.; Lieber, C. M. *Science* **2005**, *310*, 1304.
(27) Javey, A.; Nam, S.; Friedman, R. S.; Yan, H.; Lieber, C. M. *Nano Lett.* **2007**, *7*, 773.
(28) The SiNWs were transferred to the oxide surface of doped (resistivity <0.005 Ω•cm) silicon substrates (Silicon Valley Microelectronics, Inc., San Jose, CA), multiple source−drain electrodes were defined by electron beam lithography, and then Ni contacts (70 nm thick) were deposited by thermal evaporation. The contacts were annealed at 280 °C for 1 min in forming gas (10% H_2 in He).
(29) (a) Jin, S.; Whang, D.; McAlpine, M. C.; Friedman, R. S.; Wu, Y.; Lieber, C. M. *Nano Lett.* **2004**, *4*, 915. (b) Hong, W.-K.; Kim, B.-J.; Kim, T.-W.; Jo, G.; Song, S.; Kwon, S.-S.; Yoon, A.; Stach, E. A.; Lee, T. *Colloid. Surf., A* **2008**, *313*, 378.

NL802063Q